diversity

MDPI

Article

Ontogeny of Different Tetrad Types in the Single Microsporangium of *Mitrephora tomentosa* (Annonaceae)

Bingxin Li [1,2], Xiu Liu [1,3,4,5], Mei Cheng [1,4], Fengxia Xu [1,3,5,*] and Haimin Liao [6]

1 Key Laboratory of Plant Resource Conservation and Sustainable Utilization, South China Botanical Garden, Chinese Academy of Sciences, Guangzhou 510650, China; lbx353683714@163.com (B.L.); liuxiu@scbg.ac.cn (X.L.); 13064275729@163.com (M.C.)
2 National Park Research Center, School of Economics and Management, Sanming University, Sanming 365004, China
3 Center of Conservation Biology, Core Botanical Gardens, Chinese Academy of Sciences, Guangzhou 510650, China
4 College of Life Sciences, University of Chinese Academy of Sciences, Beijing 100000, China
5 Guangdong Provincial Key Laboratory of Applied Botany, South China Botanical Garden, Chinese Academy of Sciences, Guangzhou 510650, China
6 College of Life Science, Guizhou University, Guiyang 550025, China; lhaimin@163.com
* Correspondence: xfx@scbg.ac.cn

Abstract: Annonaceae, comprising approximately 107 genera and 2400 species, is the largest family among early-divergent Magnoliales. Previous studies have concentrated on the binding mechanism that holds together the four members of tetrads in Annonaceae. However, the development mechanisms of different tetrad types remain largely unknown. *Mitrephora tomentosa* was found to exhibit five permanent tetrad types, with two or three of them existing in the same microsporangium, which is ideal for studying the formation mechanisms of different permanent tetrad pollens in a single microsporangium and explaining the relationship between cytokinesis and pollen tetrad types. The ontogenetic development of the different tetrads in *M. tomentosa* was investigated using electron microscopy technologies, histochemical staining, and immunocytochemistry. During meiosis, pollen mother cells produce decussate and tetragonal tetrads by successive cytokinesis and produce tetrahedral and rhomboidal tetrads by simultaneous cytokinesis. Bidirectional callose deposition was observed in tetrahedral, tetragonal, rhomboidal, and decussate tetrads. The variations in the process of microsporogenesis randomly accumulate and manifest as different combinations of cytokinesis and callose deposition, leading to the formation of differently shaped tetrads. In mature permanent tetrad pollens, four microspores are connected by both simple cohesion and cytoplasmic channels, which also play an important role in maintaining the synchronization of the tetrad members.

Keywords: binding mechanism; cytokinesis; microsporogenesis; *Mitrephora*; tetrad pollen

check for updates

Citation: Li, B.; Liu, X.; Cheng, M.; Xu, F.; Liao, H. Ontogeny of Different Tetrad Types in the Single Microsporangium of *Mitrephora tomentosa* (Annonaceae). *Diversity* **2023**, *15*, 898. https://doi.org/10.3390/d15080898

Academic Editors: Mario A. Pagnotta and Michael Wink

Received: 19 June 2023
Revised: 27 July 2023
Accepted: 27 July 2023
Published: 29 July 2023

1. Introduction

Pollen is the male gametophyte of seed plants and plays a crucial role in plant reproduction and evolution. Pollen dispersal units exhibit impressive morphological variation in flowering plants, ranging from monads (single grains) to compound pollens (two or more grains united), which exist in over 100 families across basal angiosperms, monocots, and eudicots, and are typed with dyads, tetrads, polyads, massula, and pollinia [1–3]. As the most common form of compound pollen, tetrad pollen appears in more than 50 families [3–6]. According to the spatial arrangement of four members within the tetrad, permanent tetrads are typed as tetrahedral, tetragonal, rhomboidal, decussate, T-shape, or linear-shape [7]. Tetrad shape variation has been of long-standing interest for studies of microsporogenesis and systematics in angiosperms [6,8–10].

During microsporogenesis, the cytokinesis type and callose deposition direction show great diversity in the stage of meiosis. Generally, three types of cytokinesis, viz., successive,

simultaneous, and intermediate cytokinesis, have been recognized in angiosperms. The direction of callose deposition can be divided into centripetal and centrifugal formations. Successive cytokinesis with centrifugal callose deposition is common in monocots and basal angiosperms, and it often produces tetragonal and decussate tetrads [11–14]. Meanwhile, simultaneous cytokinesis with centripetal callose deposition is predominant in eudicots and is usually associated with tetrahedral, or rarely with rhomboidal, tetrads [15,16]. Intermediate cytokinesis is rare and has only been reported in some cycads and magnolias [17–21]. The cytokinesis type and the tetrad shape are relatively conserved in monocots and eudicots; therefore, the cytokinesis type can usually be inferred from the tetrad shape [6]. By contrast, in basal angiosperms, e.g., Magnoliaceae Juss. [22], Annonaceae Juss. [21], and Monimiaceae Juss. [23], three cytokinesis types occur, showing dramatic variation in tetrad shape, and the relationship is obscure between the type of cytokinesis and tetrad shape [24].

The tropical flowering plant family Annonaceae, with approximately 107 genera and 2400 species [25,26], is the largest family in early-divergent Magnoliales Bromhead. [27]. The monad is inferred as plesiomorphic for Annonaceae, with compound pollen (tetrads and larger polyads) derived in several phylogenetically disparate lineages [28]. Roughly 40 genera of this family shed their pollen grains in permanent tetrads, although dyads and polyads occasionally occur [2,3]. Especially, different tetrad types can occur in a single flower (*Pseuduvaria trimera* (Craib) Y.C.F. Su & R.M.K. Saunders) [21] or even in the same microsporangium (*Mitrephora tomentosa* Hook. f. & Thomson). Previous studies have concentrated on the binding mechanism holding the four members of tetrads together in Annonaceae [29–33], while the development mechanisms of different tetrad types remain largely unknown. Here, we investigated the stamens of *M. tomentosa* in different developmental stages, especially focusing on the cytokinesis type and the microspore wall formation pattern during microsporogenesis, by using electron microscopy technologies, histochemical staining, and immunocytochemistry. The present study aims to reveal the formation patterns of different tetrad types within a single microsporangium, identify the cohesion mechanism between the individual microspores within the tetrads at both the morphological and cytological levels in Annonaceae, and provide new insights into the diversity of microsporogenesis during angiosperm evolution.

2. Material and Methods

2.1. Plant Materials

Adult trees of *M. tomentosa* were located in the South Botanical Garden of the Chinese Academy of Sciences, Guangdong Province, China (113.373° N, 23.188° E). The buds and mature flowers from differentiation up to anther dehiscence were collected and fixed immediately in formalin acetic alcohol (FAA (v/v): 70% alcohol, formaldehyde, and glacial acetic acid at a ratio of 18:1:1) during the period of November 2018 to March 2019. Voucher specimens were also deposited at the South China Botanical Garden (IBSC). Classification of premeiotic PMC shapes was carried out using the length-to-width ratio, following Penet (2012) [10], which classified them as circular (ratio = 1.00), elliptic-circular (1.01–1.13), subelliptic (1.14–1.32), or elliptic (1.33–2). The palynological terminologies used here follow Halbritter et al. (2018) [34]. More than 1000 pollen grains were counted and repeated three times from 10 trees and over 100 flowers.

2.2. Scanning Electron Microscopy (SEM)

For pollen morphology observation, stamens of three mature flowers fixed in FAA were washed three times with 0.1 M phosphate-buffered saline (PBS), dehydrated in an ethanol series, and critical-point-dried. Then, the pollen sacs of the anther were dissected carefully with a tweezer and needle in order to release the pollen grains from the sacs. Pollen grains were placed directly onto brass stubs, coated with gold using a JFC-1600 Auto Fine Coater, and subjected to observations under a JSM-6360 LV (JEOL, Tokyo, Japan) SEM operated at 25 KV.

2.3. Light Microscopy (LM)

Stamens of young buds and mature flowers were fixed in FAA, dehydrated in an ethanol series, and embedded in paraffin. The embedded specimen blocks were sectioned at 8 μm on a rotary Leica microtome. Sections were stained with Ehrlich hematoxylin and were observed with a DM5500B microscope (Leica, Germany).

Stamens of different stages were also fixed in 2.5% glutaraldehyde (w/v) in 0.1 M phosphate buffer at a pH of 7.2 overnight at 4 °C and then washed three times in phosphate-buffered saline (PBS). Samples were postfixed in 2% w/v osmium tetroxide for 4 h and then washed six times in PBS for 2 h. The specimens were dehydrated in an ethanol series, embedded in Spurr resin, and sectioned at 1 μm with glass knives on an LKB-1180 microtome. Semi-thin sections were stained with toluidine blue and PAS, respectively, and observed under an LM (Leica, DM5500B).

2.4. Transmission Electron Microscopy (TEM)

The sample blocks of resin-embedded specimens were sectioned at 70 nm by a Lecia-Ultracut S ultramicrotome with a diamond knife. Ultrathin sections were stained with uranyl acetate and lead citrate and observed under a Tecnai G2 Spirit Bio TWIN TEM (FEI, Hillsboro, OR, USA).

2.5. Confocal Laser Scanning Microscopy (CLSM)

Stamens fixed in FAA were dehydrated in an ethanol series and then embedded in paraffin. Embedded blocks were sectioned at 10 μm and stained with 50 $\mu g \cdot mL^{-1}$ propidium iodide (PI) and 0.01% aniline. After dyeing for 10 min, a CLSM ZEISS 510 Meta (Zeiss, Jena, Germany) was used to observe and photograph the samples; laser wavelengths of 538 and 405 nm were used for PI and aniline blue, respectively.

3. Results

The *M. tomentosa* has five types of tetrad pollen, which are tetrahedral, tetragonal, rhomboidal, decussate, and T-shape (Figure 1), and they are all inaperturate. The tetrahedral tetrads are the most common, accounting for about 41% of the total (Figure 1a), while rhomboidal (23%) (Figure 1c), tetragonal (22%) (Figure 1b), decussate (10%) (Figure 1d), and T-shaped tetrads (4%) (Figure 1e) appear less often.

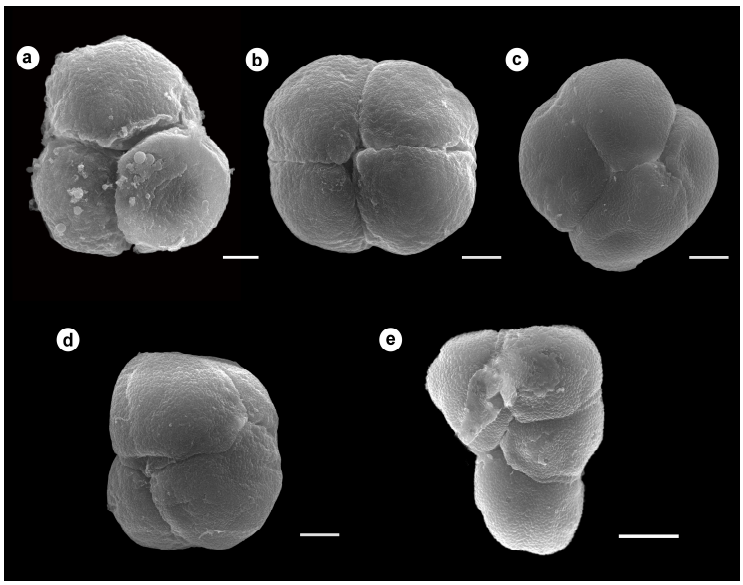

Figure 1. SEM views of different types of tetrad pollens of *M. tomentosa*. (**a**) Tetrahedral tetrad pollen. (**b**) Tetragonal tetrad pollen. (**c**) Rhomboidal tetrad pollen. (**d**) Decussate tetrad pollen. (**e**) T-shape tetrad pollen. Scale bar: (**a**–**d**) 10 μm; (**e**) 20 μm.

3.1. Pollen Mother Cell Stage

Flower buds of *M. tomentosa* were entirely enclosed by a brown calyx ca. 5–8 mm in diameter, and the stamens were about 0.8–1 mm in diameter (Figure 2a). Pollen development started with the differentiation of pollen mother cells (PMCs) and was kept synchronous within the individual microsporangium (Figure 3a,d,f). Early in development, the polygonal PMCs with a large nucleus were appressed against each other (Figure 3a) and connected by cytoplasmic channels, which were formed by incomplete separation of the cytoplasm at the connection area (Figure 3b). In the meantime, there was no callose wall wrapping around the PMCs (Figure 3c). As the PMC stage progressed, the intercellular spaces among the PMCs were gradually enlarged (Figure 3d), and the PMCs were surrounded by a special callose envelope (Figure 3e). Before meiosis and cytokinesis were initiated, PMCs were elliptic, and division furrows began to deposit on the periphery of the cell wall of the PMCs (Figure 3f).

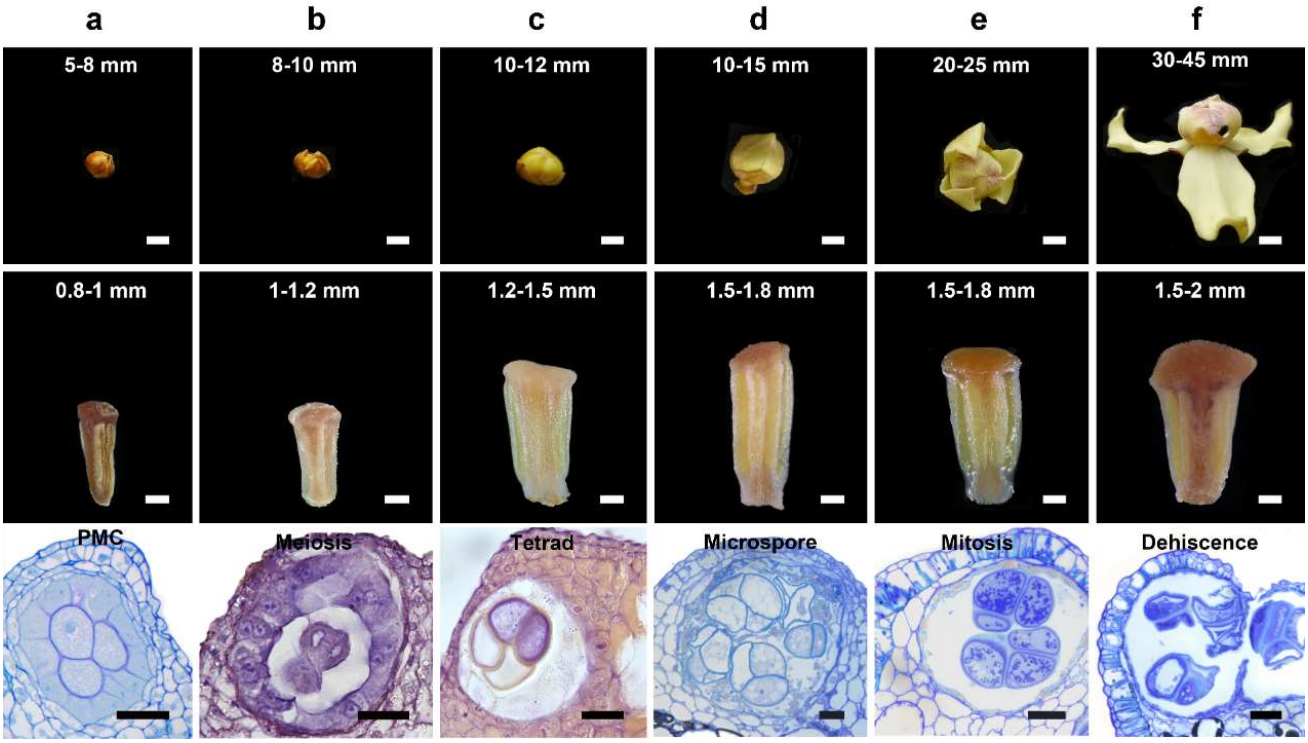

Figure 2. Different developmental stages of the flower buds and anthers of *M. tomentosa*. (**a**) Young flower bud and anther of the PMC stage. (**b**) Flower bud and anther of the meiosis stage. (**c**) Flower bud and anther of the tetrad stage. (**d**) Flower bud and anther of the unicellular microspore stage. (**e**) Flower bud and anther of the bicellular pollen stage. (**f**) Mature flower and anther of mature pollen stage. Scale bars: all flower buds at 5 mm; all anthers observed under light microscope at 200 μm; all sections of anther at 30 μm.

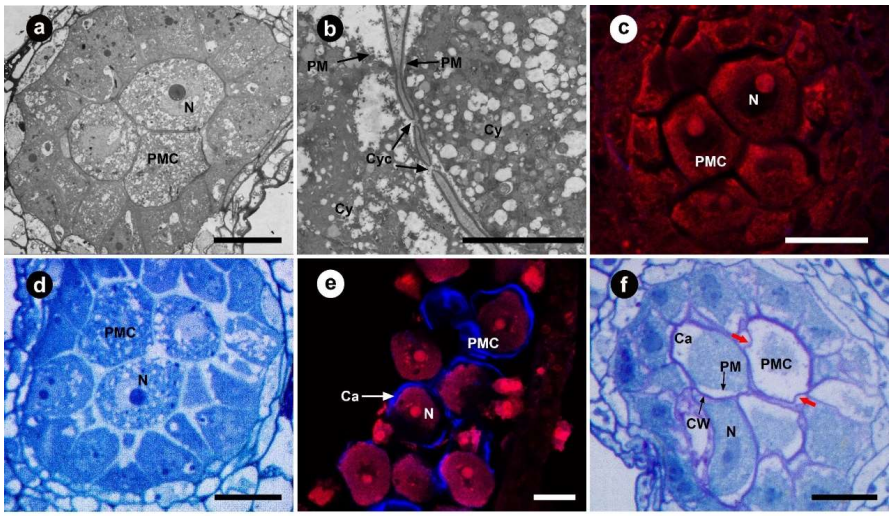

Figure 3. PMC stage. (**a**) PMCs are polygonal in shape. (**b**) Adjacent PMCs are connected by cytoplasmic channels (arrows). (**c**) Callose has not deposited at the walls of the PMCs. (**d**) Gap formed between PMCs. (**e**) PMC surrounded by a special callose envelope. (**f**) Premeiotic PMCs are elliptic, and division furrows (arrows) start to appear at the periphery of walls of the PMCs. (**a**,**b**): TEM view. (**c**,**e**): CLSM images of nucleus and callose detected by PI and aniline blue. (**d**,**f**): Semi-thin sections stained with toluidine blue. *CLSM*: confocal laser scanning microscopy, *Ca*: callose, *Cy*: cytoplasm, *Cyc*: cytoplasmic channel, *CW*: cell wall of the pollen mother cell, *N*: nucleus, *PI*: propidium iodide, *PM*: plasmalemma, *PMC*: pollen mother cell, *TEM*: transmission electron microscopy. Scale bars: (**a**,**c**,**d**–**f**): 20 μm; (**b**): 500 nm.

3.2. Meiosis Stage

With the flower buds expanded slightly (ca. 8–10 mm), the brown calyx lobes divided, and the anthers elongated to ca. 1–1.2 mm (Figure 2b). Before meiosis and cytokinesis were initiated, the callose walls surrounding the PMCs were gradually thickened (Figure 4a). Each PMC undergoes two meiotic divisions and produces four meiotic nuclei (Figure 4b,c,l). Both successive and simultaneous cytokinesis were observed not only in the different anther lobules but also in the same microsporangiums (Figure 4k,l). A temporary dyad is characteristic of successive cytokinesis, while four nuclei being in the same cytoplasm is characteristic of simultaneous cytokinesis. In PMCs with successive cytokinesis, the four meiotic nuclei are arranged in multiplanar (decussate in Figure 4d,e) or uniplanar (tetragonal in Figure 4c,f) formation. In addition, cytoplasmic division occurred twice. The first one occurred after the end of meiosis I, when a cleavage plane of callose formed centripetally and orthogonally to the spindle between the two sister meiotic nuclei produced by meiosis I, resulting in a temporary dyad (Figure 4b,c). The second one occurred after meiosis II, and two callose plates bidirectionally formed, corresponding to a decussate tetrad (Figure 4d,e) and a tetragonal tetrad (Figure 4c,f) with two callose plates, respectively. In PMCs with simultaneous cytokinesis, four meiotic nuclei are arranged in a multiplanar tetrahedral (Figure 4g) or uniplanar rhomboidal (Figure 4h) formation, and cytoplasmic division does not occur until the four nuclei form after the end of meiosis II (Figure 4g–i). Six or five callose plates formed perpendicular to the meiotic spindle, connecting the four daughter nuclei (Figure 4g–i); as a result, tetrahedral (Figure 4g), and rhomboidal tetrads (Figure 4h,i) formed. Therefore, except for T-shape tetrad (Figure 4j), the other four tetrad types, i.e., decussate, tetragonal, rhomboidal, and tetrahedral, all exhibit bidirectional deposition of callose walls. Decussate and tetragonal tetrads form in simultaneous cytokinesis, while rhomboidal and tetrahedral tetrads form in successive cytokinesis.

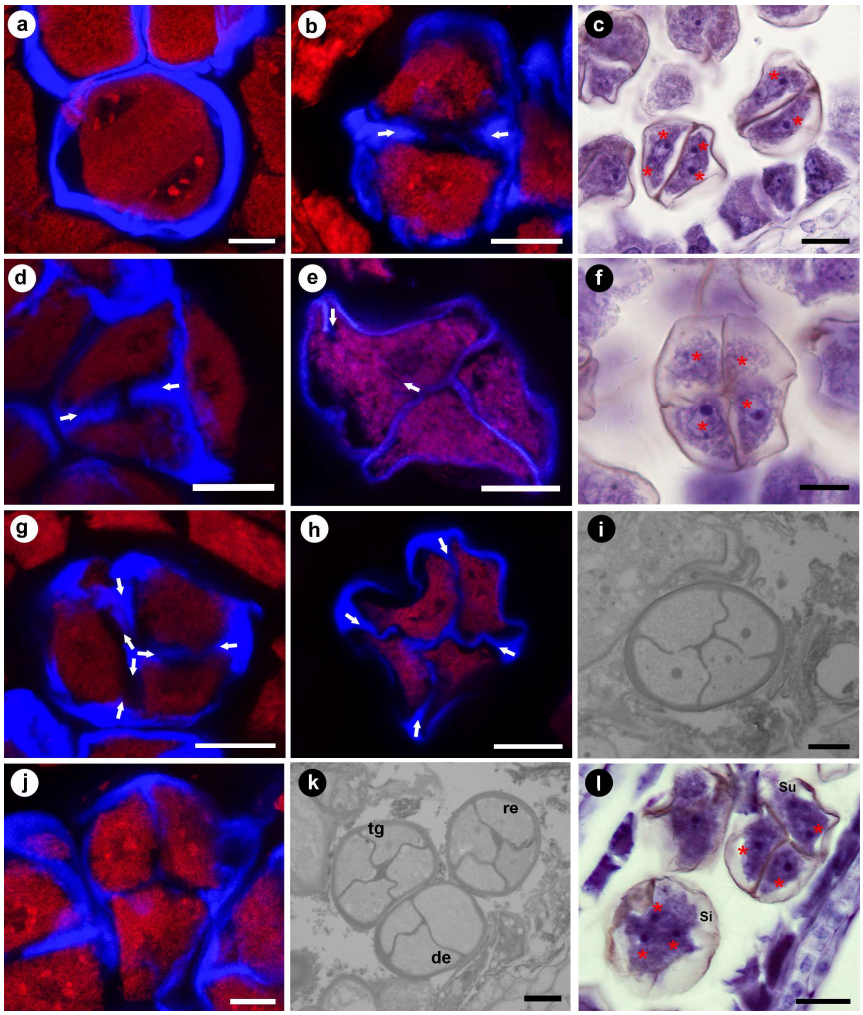

Figure 4. Meiosis stage. (**a**) PMCs during meiosis anaphase I surrounded by thick callose. (**b**–**f**) Successive microsporogenesis. (**b**) Callose plate centripetally formed with successive cytokinesis. (**c**) A temporary dyad was formed. (**d**) Decussate tetrad with two callose plates at second cytoplasmic division; only one plate was observed with bidirectional deposition in the section. (**e**) After meiosis II, two callose plates bidirectionally formed in decussate tetrads. (**f**) Tetragonal tetrad with three callose plates after second cytoplasmic division. (**g**–**i**) Simultaneous microsporogenesis. (**g**) Tetrahedral tetrad with six callose plates formed via simultaneous cytokinesis; only three plates were observed in the section. (**h**,**i**) Rhomboidal tetrad with five callose plates formed via simultaneous cytokinesis. (**j**) T-shape tetrad just after the completion of cell plate formation. (**k**) Decussate, tetragonal, and rhomboidal tetrads in a single microsporangium. (**l**) Successive and simultaneous cytokinesis concurrently appeared in the same microsporangium. Asterisks refer to locations of the meiotic nuclei, and arrows denote the orientation of the callose deposition. *Si*: simultaneous cytokinesis, *Su*: successive cytokinesis. (**a**,**b**,**d**,**e**,**g**,**h**,**j**): Confocal laser scanning microscopy images of nucleus and callose. Blue fluorescence: callose, red fluorescence: nucleus and cytoplasm. (**c**,**l**): Light microscopy images of paraffin sections stained with Ehrlich hematoxylin. (**i**–**k**): Light microscopy images of semi-thin sections stained with toluidine blue. Scale bars: (**a**,**b**,**d**–**k**): 10 μm; (**c**,**l**): 15 μm.

3.3. Tetrad Stage

Flower buds enlarged to ca. 10–12 mm and changed color from brown to bright yellow. The anther length was ca. 1.2–1.5 mm (Figure 2c). After the completion of meiosis and cytokinesis, various types of meiotic tetrad were synchronously produced in the same microsporangium (Figure 5a). At the early tetrad stage, four sibling microspores within

one tetrad were encapsulated in a communal callose wall (Figure 5b–g), and a conspicuous nucleus was located at the center of the cell (Figure 5f). In the tetrads of tetrahedral, rhomboidal, and tetragonal tetrads, a thick central callose region was evident (Figure 5b–d). It is common for a portion of the outer callose envelope to be shared between neighboring PMCs, with no PMC coat present between the adjacent callose layers (Figure 5g). Adjacent microspores were separated from each other by the thick callose (Figure 5b–f) but presented narrowed channels without callose layers that were partially shared (arrow) between the neighboring tetrads (Figure 5h). Proexine began to form between the callose wall and the plasma membrane, except in the locations without callose, showing the future cytoplasmic channels between two microspores (Figure 5 h). Proexine was distributed in radial groups in the network, except in cytoplasmic channels (asterisk), which connected tetrad members within the same tetrad (Figure 5i,j). Later on, the callose wall was gradually destroyed (Figure 5k). Meanwhile, the tectum layers of adjoining microspores were fused, forming a simple cohesion held together with the tetrad members (Figure 5l). At the late tetrad stage, exines at the proximal and distal sides of the microspore are synchrogenically formed, an occurrence which is marked by the occurrence of distinct protectum, procolumellae, and profoot layers (Figure 5m,n).

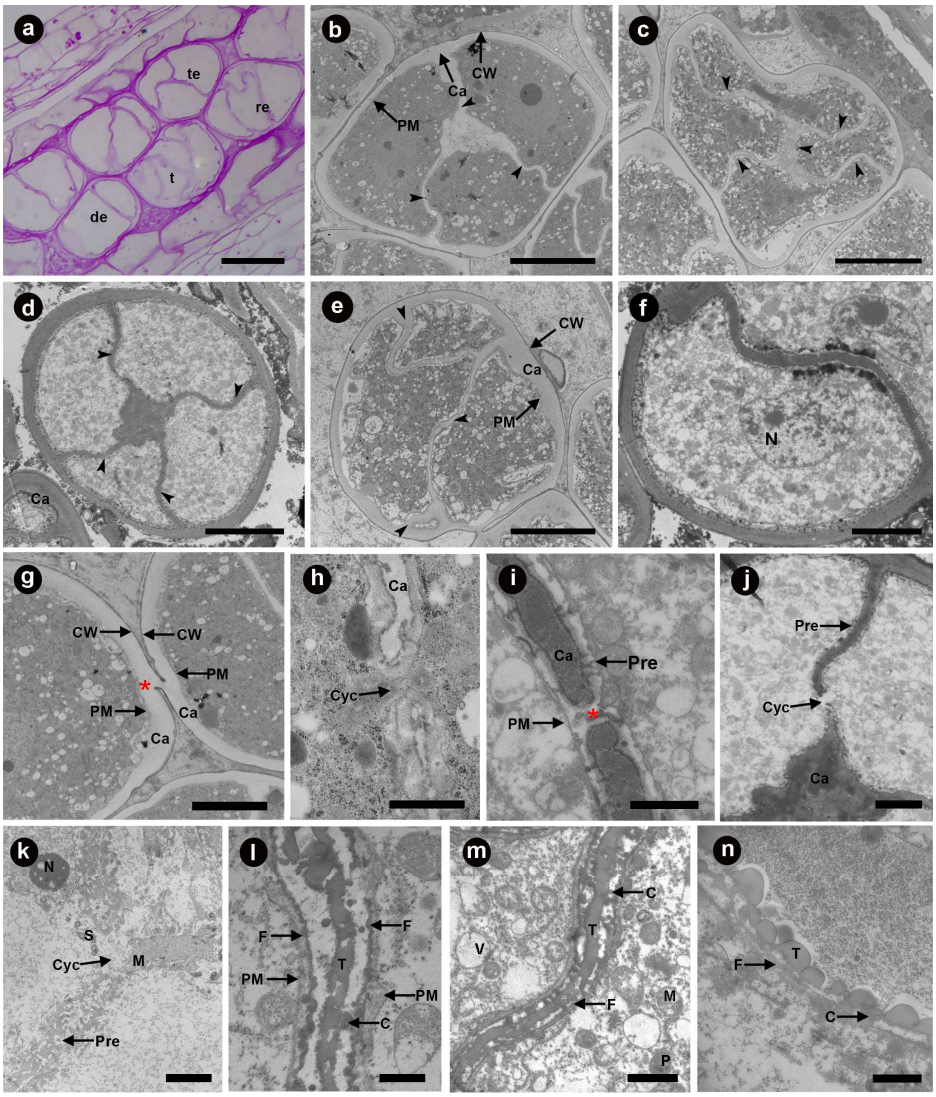

Figure 5. Tetrad stage. (**a**) Semi-thin section stained with PAS shows different tetrad types in the same microsporangium. (**b**–**f**) Uneven callose walls are deposited between the cell walls of PMCs and the plasmalemma, which encloses the tetrad, and separate the four microspores from each other.

(**b**) Tetrahedral tetrad formed six callose plates, among which three plates are visible in the section (arrowheads). (**c**) Rhomboidal tetrad formed five callose plates (arrowheads). (**d**) Tetragonal tetrad formed three callose plates (arrowheads). The thick central callose region in the tetrads was evident in (**b**–**d**). (**e**) Decussate tetrad formed three callose plates (arrowheads). (**f**) Details of microspore with a conspicuous nucleus located at the center. (**g**) The callose wall is continuous with the shared callose wall (asterisk) between two adjacent PMCs. (**h**) The cytoplasmic channel is partially shared between the neighboring tetrads. (**i**,**j**) Proexine begin to form between the callose wall and the plasma membrane, except in cytoplasmic channels (asterisk). (**k**) At the locations without callose, there is a cytoplasmic channel (arrow) through which starch grains and mitochondria are passing. (**l**,**m**) Protectum begins to fuse at the proximal side, which means a simple aggregate begins to form. (**n**) Detail of proexine at the distal side, showing protectum, procolumellae, and profoot layers. *C*: columella, *Ca*: callose, *Cyc*: cytoplasmic channel, *CW*: cell wall of PMC, *CWI*: central callose wall island, *de*: decussate tetrad, *F*: foot layer, *M*: mitochondria, *N*: nucleus, *P*: plastid, *Pre*: proexine, *PM*: plasmalemma, *re*: rhomboidal tetrad, *S*: starch, *T*: tectum, *te*: tetrahedral tetrad, t: T-shape tetrad. Scale bar: (**a**–**e**): 10 μm; (**f**,**g**): 5 μm; (**h**–**n**): 1 μm.

3.4. Unicellular, Bicellular Microspore and Mature Pollen Stage

At unicellular microspore stage, flower buds enlarged to ca. 10–15 mm. The anther length was ca. 1.5–1.8 mm (Figure 2d). The callose walls enveloping the tetrads were entirely disintegrated, but the tetrad members still maintained adhesion (Figure 6a) due to the tectum layers of adjacent microspores being greatly fused at both proximal sides (Figure 6b,c). Furthermore, intine was deposited between the foot layer and the plasmalemma (Figure 6b,c). As ontogeny proceeded, tetrad members underwent mitosis and formed a big vegetative cell at the center and a small generative cell at the edge of the microspores (Figure 6d), and pollen development entered the bicellular pollen stage. At this stage, the flower buds enlarged to ca. 20–25 mm, and the anther length was the same as in the last stage (Figure 2e). Cytoplasmic channels between the proximal sides of adjacent microspores were still observed (Figure 6e,f), and together with simple cohesion at the distal side functioned as the binding mechanism of the tetrads (Figure 6g,h). Columella layers of the microspores were not obvious in the cohesion area during the unicellular and bicellular pollen stages (Figure 6b,c,g,h). At the mature pollen stage, the petals completely opened, being ca. 30–45 mm in diameter, and the anthers were 1.5–2 mm (Figure 2f). The anthers started to dehisce (Figure 6i). Mature spheroidal pollen grains contain abundant starch grains (Figure 6j). The building of the exines and intines of the microspores was completed, and the granule appeared in the columella layer (Figure 6k,l). All types of tetrads—tetrahedral, tetragonal, rhomboidal, decussate, and T-shape—have no aperture but rather exhibit proximal thinning of the exine.

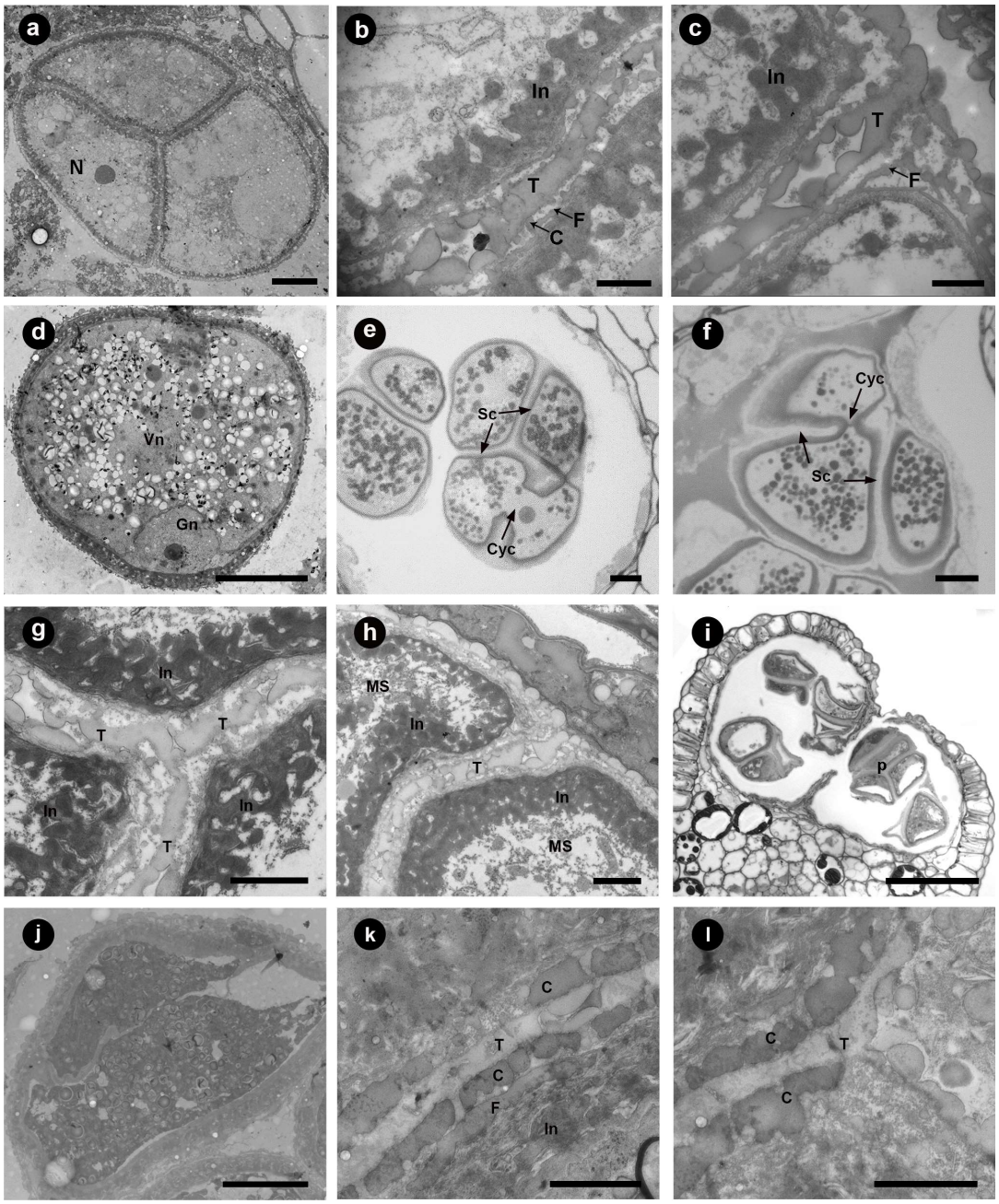

Figure 6. Unicellular microspore, bicellular microspore, and mature pollen stages. (**a**–**c**) Unicellular microspore stage. (**a**) Microspores have a conspicuous nucleus located at the center at the early unicellular microspore stage. (**b**) Simple cohesion at the proximal side of adjacent microspores. (**c**) Intine began to be deposited between the foot layer and the plasmalemma. (**d**–**h**) Bicellular microspore stage. (**d**) Vegetative cell and generative cell are visible within the bicellular microspore. (**e**) Tetragonal tetrad connected by simple cohesion and cytoplasmic channel. (**f**) Tetrahedral tetrad connected by simple cohesion and cytoplasmic channel. (**g**,**h**) Simple cohesion occurred at the proximal side (**g**) and distal side (**h**) of adjacent microspores. (**i**–**l**) Mature pollen stage. (**i**) Dehiscent anther. (**j**) Mature spheroidal pollen grains contain rich starch grains. (**k**,**l**) Tectum entirely fused, associated with simple cohesion, either on the proximal side (**k**) or distal side (**l**). *C*: columella, *Cyc*: cytoplasmic channel, *Gn*: generative cell, *F*: foot layer, *In*: intine, *MS*: microspore, *N*: nucleus, *p*: mature pollen, *Sc*: simple cohesion, *SEM*: scanning electron microscopy, *T*: tectum, *TEM*: transmission electron microscopy, *Vn*: vegetative cell. Scale bars: (**a**,**d**–**f**,**j**): 10 μm; (**b**,**c**): 1 μm; (**g**,**h**,**k**,**l**): 2 μm; (**i**): 75 μm.

4. Discussion

4.1. The Diversity of Microsporogenesis

Although both successive and simultaneous cytokinesis were observed within the same anther of *M. tomentosa*, differences between them occurred after meiosis I. A formation model of different tetrad types is illustrated in Figure 7a–d. In successive cytokinesis, a cell plate was formed after the first meiosis stage to separate the two daughter nuclei, producing a dyad temporarily. Subsequently, the second meiosis stage occurred. According to the relative position of the meiotic nuclei, new cell plates started to be deposited in decussate (Figure 7a) or tetragonal (Figure 7b) formation, corresponding to three callose plates (Figure 7a,b). However, in the simultaneous one, the second division continued after the first division without a cell plate forming and produced four meiotic nuclei in a tetrahedral shape, with six callose plates deposited (Figure 7c), or a rhomboidal shape with five callose plates (Figure 7d). Obviously, in *M. tomentosa*, the type of the tetrad was considered to be determined by the relative positions of the four meiotic nuclei together with the cytokinesis patterns and the direction of callose deposition during microsporogenesis, similar to the mechanism of tetrad formation found in *Pseuduvaria trimera* [21]. Because pollen meiotic progression is mediated by microspores and tapetum expression [35,36], and the synthesis of callose is determined exclusively by tapetum [37], we speculated that the type of tetrad formed is co-regulated by sporophytic and gametophytic factors.

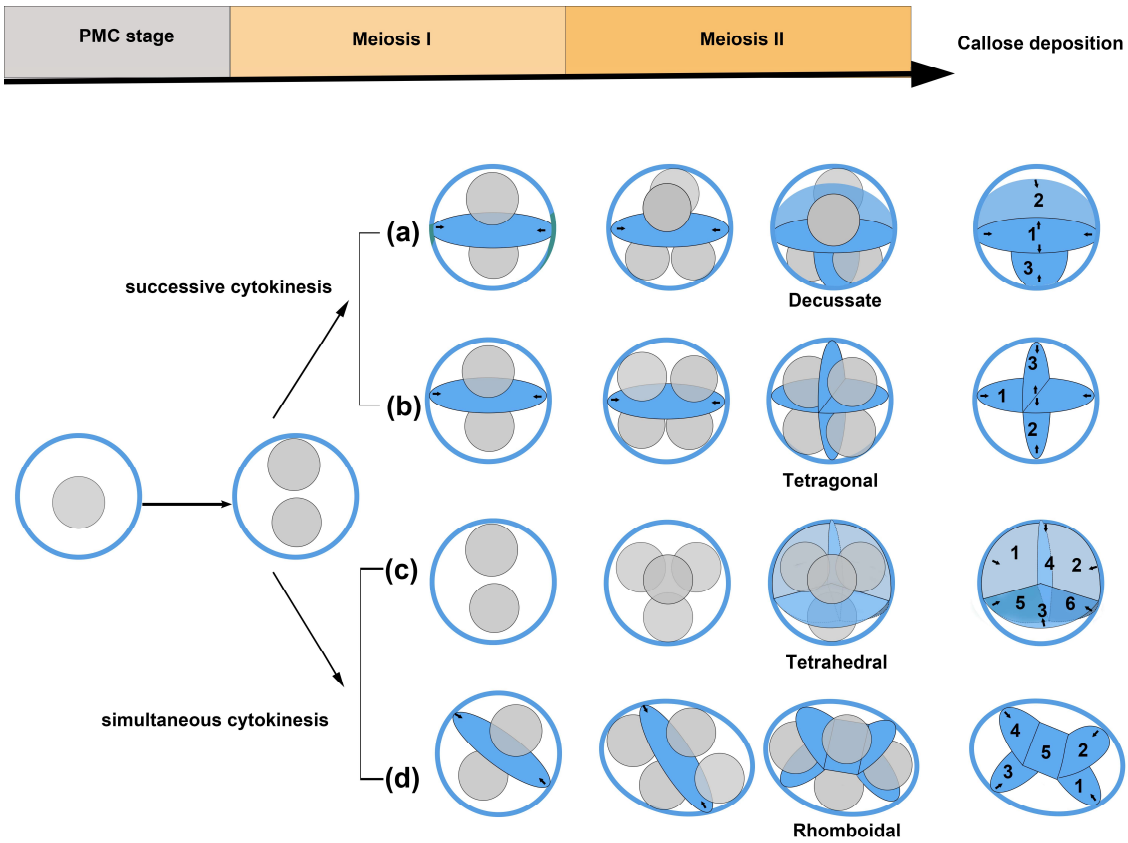

Figure 7. Tetrad configurations differ in the number of cleavage planes of callose and the orientation of meiotic nuclei during microsporogenesis in *M. tomentosa*. (**a**,**b**): Three planes for decussate (**a**) and tetragonal (**b**) formations, respectively. (**c**,**d**): Six and five planes corresponding tetrahedral (**c**) and rhomboidal tetrads (**d**). For each tetrad form, the callose deposition began at the border of the PMC and progressed towards the center of the PMC. Callose is represented by blue, and arrows indicate the direction of callose progression.

Recently, Hu et al. (2021) reported a new bidirectional callose deposition pattern in Magnoliaceae (*Magnolia denudata* Desr.), where centripetally growing callose walls fused with a concurrent callose wall island in the center of the cell during cytokinesis [38]. This pattern was also later observed in Nymphaeaceae Salisb. (*Nymphaea colorata* Peter), and the author proposed that bidirectional callose deposition may be a common and perhaps ancestral feature of microsporogenesis in some basal angiosperms [39]. In *M. tomentosa*, tetrahedral, tetragonal, rhomboidal, and decussate tetrads were produced with bidirectional callose deposition, which was the first specific report on this topic in Annonaceae. In fact, the bidirectional pattern was shown in earlier studies of *Pseuduvaria trimera* but was not mentioned at that time [21]. Moreover, bidirectional callose deposition was observed in early research on Euphorbiaceae Juss. (*Codiaeum variegatum* (L.) Blume), Asteraceae Martinov (*Catananche caerulea* L.), Arecaceae Bercht. & J. Presl (*Copernicia hospita* Mart.), Onagraceae Juss. (*Epilobium roseum* Schreb.), and Linaceae DC. ex Perleb (*Reinwardtia cicanoba* Hara), but it was also ignored by the authors [8,9,40–42]. Obviously, bidirectional callose deposition is widespread in angiosperms, rather than being confined to basal angiosperms as Wu et al. (2021) expected [39]. It is worthwhile to further discuss whether bidirectional callose deposition independently originated in angiosperms.

Pollen morphogenesis in angiosperms exists in a state of long-term evolutionary stasis, mainly due to the selection pressure acting on the aperture pattern. Several studies have demonstrated that pollen aperture pattern ontogeny is determined by the microsporogenesis process [8,13,40,43,44]. As a result, triaperturate pollens are widely dominant in eudicots and are produced by a conserved microsporogenesis process, i.e., simultaneous cytokinesis combined with centripetal callose deposition [9,15,42,45,46]. Monosulcate pollens are produced predominantly in basal angiosperms and monocots, which is a consequence of successive cytokinesis and centrifugal callose deposition [47,48]. However, in some angiosperm species with global aperture or inaperturate pollens, the process of microsporogenesis displays great diversity and exhibits different combinations of cytokinesis type and callose deposition direction, resulting in different shapes of tetrads, e.g., in Euphorbiaceae (*Baloghia inophylla* (G. Forst.) P.Green), Apocynaceae Juss. (*Apocynum cannabinum* L.), Linaceae (*Reinwardtia cicanoba*), Malvaceae Juss. (*Hibiscus waimeae* A. Heller), Orobanchaceae Vent. (*Orobanche hederae* Duby), and Plantaginaceae Juss. (*Plantago lanceolata* L.) [9,46,48]. In Annonaceae, inaperturate pollens predominate, and the process of microsporogenesis displays great diversity; simultaneous or intermediate cytokinesis combine with centripetal or bidirectional callose deposition and form tetrahedral tetrads in *Cymbopetalum* Benth., *Pseudoxandra* R.E. Fr., *Pseuduvaria* Miq., and *Mitrephora* Hook. f. & Thomson, which are similar to eudicots ([4,21,30], this study), and successive cytokinesis combined with centrifugal callose deposition produces tetragonal tetrads in *Xylopia* that are similar to monocots [49]. More diversified combinations, for example, of successive cytokinesis combined with centripetal or bidirectional callose deposition produce tetragonal tetrads in *Annona* L., *Asimina* Adans., and *Mitrephora* ([49,50], this study). Hence, the cytokinesis type is highly labile in Annonaceae, and it is difficult to predict the cytokinesis type from tetrad configurations. We suggest that variations in the process of microsporogenesis randomly accumulate and manifest as different combinations of cytokinesis and callose deposition, and consequently, the formation of differently shaped tetrads.

4.2. Cohesion Mechanism of the Permanent Tetrad Pollen

In most members of Annonaceae, the formation of permanent tetrad pollens is connected by various microspore cohesion mechanisms, and therefore, adjacent microspores within the tetrad fail to dissociate [21,29,31,32,51,52]. Four connecting types have been reported in Annonaceae, viz. cytoplasmic channels, simple cohesion, callose–cellulose binding, and crosswall cohesion [21,29,31,52], among which both cytoplasmic channels and simple cohesion were observed in this study (Figure 6e–h).

Cytoplasmic channels have not only been observed in Annonaceae connecting permanent tetrad pollens ([21], this study). In *Victoria* Lindl. (Nymphaeaceae) with shed

polyad pollen [53], however, there is no evidence of cytoplasmic channels that connect the two adjacent microspores. Instead, cytoplasmic channels are transient and serve as substructures for the wall bridge [53]. Moreover, in a few cases of cytoplasmic channels appearing together with another binding mechanism, e.g., cytoplasmic channels with simple cohesion in Ericaceae Juss. [54] and cytoplasmic channels with crosswall cohesion in Nymphaeaceae [53,54], cytoplasmic channels were hypothesized to act as a template for proexine deposition due to these channels temporarily appearing from meiosis to the tetrad stage but disappearing with the deposition of pollen proexine [53,54].

In *M. tomentosa*, both a communal callose wall and cytoplasmic channels formed at the proximal side, surrounding the individual tetrad and also holding tetrad members together with each other at the early tetrad stage. At the late tetrad stage, when the callose wall was degraded, tetrad members were connected by simple cohesion resulting from the fused tectum of an adjoining microspore at the proximal side. Although the cytoplasmic channels persisted from the early tetrad stage to the mature pollen stage, they were not the only microspore cohesion method, nor did they provide a template for exine deposition, as in Ericaceae and Nymphaeaceae. In Annonaceae, we considered that the cytoplasmic channels provide some communication between adjacent tetrad members, e.g., via organelles or substances ([21], this study), and play an important role in maintaining synchronization in addition to connecting the four microspores during tetrad pollen development.

5. Conclusions

Mitrephora tomentosa was observed to exhibit both successive and simultaneous cytokinesis in the same microsporangium. During meiosis, pollen mother cells produce decussate and tetragonal tetrads by successive cytokinesis and produce tetrahedral and rhomboidal tetrads by simultaneous cytokinesis combined with bidirectional callose deposition. The variations in the process of microsporogenesis randomly accumulate and manifest as different combinations of cytokinesis and callose deposition, forming differently shaped tetrads. In *M. tomentosa* tetrad pollens, four microspores are connected by both simple cohesion and cytoplasmic channels, which also play an important role in maintaining the synchronization of the tetrad members.

Author Contributions: F.X. and H.L. designed the study. B.L., X.L. and M.C. performed the experiments and conducted all data analyses. All listed authors contributed to the revision and optimization of the drafted paper. All authors have read and agreed to the published version of the manuscript.

Funding: This work was financially supported by the National Natural Science Foundation of China (31970188), the Natural Science Foundation of Fujian Province of China (2022J011187), the Cultivation Project of the National Natural Science Foundation in Sanming University (KD210008P), and the Start-up Foundation for Advanced Talents in Sanming University (RD21002P).

Institutional Review Board Statement: Not applicable.

Data Availability Statement: Not applicable.

Acknowledgments: We are grateful to Xinlan Xu, Xiaoying Hu, and Rufang Deng (South China Botanical Garden, Chinese Academy of Sciences) for their technical assistance with the CLSM, SEM, and TEM. We also thank Yongmei Zhang for providing Figure 1e.

Conflicts of Interest: The authors declare no conflict of interest.

References

1. Erdtman, G. *Pollen Morphology and Plant Taxonomy. Angiosperms. An Introduction to Palynology I*; Hafner Publishing: New York, NY, USA, 1966.
2. Copenhaver, G.P. A compendium of plant species producing pollen tetrads. *J. N. Carol. Acad. Sci.* **2005**, *121*, 17–35.
3. Walker, J.W. Pollen morphology, phytogeography, and phylogeny of the *Annonaceae*. *Contrib. Gray Herb. Harv. Univ.* **1971**, *202*, 1–130. [CrossRef]
4. Walker, J.W. Contributions to the pollen morphology and phylogeny of the *Annonaceae* I. *Grana* **1971**, *11*, 45–54. [CrossRef]
5. Zhang, M.Y.; Lu, L.; Wortley, A.H.; Wang, H.; Li, D.Z.; Blackmore, S. Evolution of angiosperm pollen. 4. The basal angiosperms. *Ann. Mo. Bot. Gard.* **2017**, *102*, 141–182. [CrossRef]

6. Furness, C.A.; Rudall, P.J.; Sampson, F.B. Evolution of Microsporogenesis in Angiosperms. *Int. J. Plant Sci.* **2002**, *163*, 235–260. [CrossRef]
7. Erdtman, G. *Handbook of Palynology. Morphology, Taxonomy, Ecology. An Introduction to the Study of Pollen Grains and Spores*; Hafner: New York, NY, USA, 1969.
8. Albert, B.; Nadot, S.; Dreyer, L.; Ressayre, A. The influence of tetrad shape and intersporal callose wall formation on pollen aperture pattern ontogeny in two eudicot species. *Ann. Bot.* **2010**, *106*, 557–564. [CrossRef]
9. Matamoro-Vidal, A.; Furness, C.A.; Gouyon, P.H.; Wurdack, K.J.; Albert, B. Evolutionary stasis in Euphorbiaceae pollen: Selection and constraints. *J. Evol. Biol.* **2012**, *25*, 1077–1096. [CrossRef]
10. Penet, L. Premeiotic microsporocyte cell shape influences shape of tetrads during microsporogenesis. *Int. J. Plant Sci.* **2012**, *173*, 375–381. [CrossRef]
11. Albert, B.; Toghranegar, Z.; Nadot, S. Diversity and evolution of microsporogenesis in Bromeliaceae. *Bot. J. Linn. Soc.* **2014**, *176*, 36–45. [CrossRef]
12. Nadot, S.; Furness, C.A.; Sannier, J.; Penet, L.; Triki-Teurtroy, S.; Albert, B.; Ressayre, A. Phylogenetic comparative analysis of microsporogenesis in angiosperms with a focus on monocots. *Am. J. Bot.* **2008**, *95*, 1426–1436. [CrossRef]
13. Ressayre, A.; Godelle, B.; Raquin, C.; Gouyon, P.H. Aperture pattern ontogeny in angiosperms. *J. Exp. Zool.* **2002**, *294*, 122–135. [CrossRef] [PubMed]
14. Penet, L.; Nadot, S.; Ressayre, A.; Forchioni, A.; Dreyer, L.; Gouyon, P.H. Multiple developmental pathways leading to a single morph: Monosulcate pollen (examples from the *Asparagales*). *Ann. Bot.* **2005**, *95*, 331–343. [CrossRef] [PubMed]
15. Nadot, S.; Forchioni, A.; Penet, L.; Sannier, J.; Ressayre, A. Links between early pollen development and aperture pattern in monocots. *Protoplasma* **2006**, *228*, 55–64. [CrossRef] [PubMed]
16. Ressayre, A. Equatorial aperture pattern in monocots: Same definition rules as in eudicots? The example of two species of Pontederiaceae. *Int. J. Plant Sci.* **2001**, *162*, 1219–1224. [CrossRef]
17. Ouyang, H.B.; Li, Y.; Zhang, S.Z.; Li, N.; Wu, H. Microsporogenesis of *Cycas elongata* and its systematic implication. *Acta Bot. Sin.* **2004**, *42*, 500–512. (In Chinese)
18. Yan, X.; Bai, M.; Ning, X.; Ouyang, H.; Zhang, S.; Yang, M.; Wu, H. Spatiotemporal features of microsporogenesis in the cycad species *Macrozamia communis*. *Am. J. Bot.* **2015**, *102*, 1061–1072. [CrossRef]
19. Zhang, H.F.; Ouyang, H.B.; Du, J.Y.; Zhang, S.Z.; Li, Y.; Wu, H. Microsporogenesis of *Cycas* and its systematic implications. *J. Syst. Evol.* **2012**, *50*, 125–134. [CrossRef]
20. Galati, B.; Zarlavsky, G.; Rosenfeldt, S.; Gotelli, M. Pollen ontogeny in *Magnolia liliflora* Desr. *Plant Syst. Evol.* **2011**, *298*, 527–534. [CrossRef]
21. Li, B.X.; Xu, F.X. Formation pattern in five types of pollen tetrad in *Pseuduvaria trimera* (*Annonaceae*). *Protoplasma* **2019**, *256*, 53–68. [CrossRef]
22. Xu, F.X.; Chen, D.Q.; Specht, C. Comparative microsporogenesis and anther development of selected species from Magnoliaceae. *Nord. J. Bot.* **2013**, *31*, 291–300. [CrossRef]
23. Sampson, F.B. Studies on the Monimiaceae. *Aust. J. Bot.* **1969**, *17*, 403–424. [CrossRef]
24. Rudall, P.J.; Furness, C.A.; Chase, M.W.; Fay, M.F. Microsporogenesis and pollen sulcus type in *Asparagales* (*Lilianae*). *Canadian J. Bot.* **1997**, *75*, 408–430. [CrossRef]
25. Chatrou, L.W.; Pirie, M.D.; Erkens, R.H.J.; Couvreur, T.L.P.; Neubig, K.M.; Abbott, J.R.; Mols, J.B.; Maas, J.W.; Saunders, R.M.K.; Chase, M.W. A new subfamilial and tribal classification of the pantropical flowering plant family *Annonaceae* informed by molecular phylogenetics. *Bot. J. Linn. Soc.* **2012**, *169*, 5–40. [CrossRef]
26. Guo, X.; Tang, C.C.; Thomas, D.C.; Couvreur, T.L.P.; Saunders, R.M.K. A mega-phylogeny of the *Annonaceae*: Taxonomic placement of five enigmatic genera and support for a new tribe, Phoenicantheae. *Sci. Rep.* **2017**, *7*, 7323. [CrossRef]
27. APG IV. An update of the Angiosperm phylogeny group classification for the orders and families of flowering plants: APG IV. *Bot. J. Linn. Soc.* **2016**, *181*, 1–20. [CrossRef]
28. Xue, B.; Guo, X.; Landis, J.B.; Sun, M.; Tang, C.C.; Soltis, P.S.; Soltis, D.E.; Saunders, R.M.K. Accelerated diversification correlated with functional traits shapes extant diversity of the early divergent angiosperm family *Annonaceae*. *Mol. Phylogenet. Evol.* **2020**, *142*, 106659. [CrossRef] [PubMed]
29. Tsou, C.H.; Fu, Y.L. Tetrad pollen formation in *Annona* (*Annonaceae*): Proexine formation and binding mechanism. *Am. J. Bot.* **2002**, *89*, 734–747. [CrossRef]
30. Tsou, C.H.; Fu, Y.L. Octad pollen formation in *Cymbopetalum* (*Annonaceae*): The binding mechanism. *Plant Syst. Evol.* **2007**, *263*, 13–23. [CrossRef]
31. Su, Y.C.F.; Saunders, R.M.K. Pollen structure, tetrad cohesion and pollen-connecting in *Pseuduvaria* (*Annonaceae*). *Bot. J. Linn. Soc.* **2003**, *143*, 69–78. [CrossRef]
32. Lora, J.; Testillano, P.S.; Risueno, M.C.; Hormaza, J.I.; Herrero, M. Pollen development in *Annona cherimola* Mill. (*Annonaceae*). Implications for the evolution of aggregated pollen. *Bmc Plant Biol.* **2009**, *9*, 129. [CrossRef] [PubMed]
33. Lora, J.; Herrero, M.; Hormaza, J.I. Microspore development in *Annona* (*Annonaceae*): Differences between monad and tetrad pollen. *Am. J. Bot.* **2014**, *101*, 1508–1518. [CrossRef]
34. Halbritter, H.; Silvia, U.; Grímsson, F.; Weber, M.; Frosch-Radivo, A. *Illustrated Pollen Terminology*, 2nd ed.; Springer: Cham, Switzerland, 2018.

35. Tidy, A.C.; Ferjentsikova, I.; Vizcay-Barrena, G.; Liu, B.; Yin, W.Z.; Higgins, J.D.; Xu, J.; Zhang, D.B.; Geelen, D.; Wilson, Z.A. Sporophytic control of pollen meiotic progression is mediated by tapetum expression of *Aborted microspores*. *J. Exp. Bot.* **2022**, *73*, 5543–555840. [CrossRef] [PubMed]
36. Ma, X.F.; Wu, Y.; Zhang, G.F. Formation pattern and regulatory mechanisms of pollen wall in *Arabidopsis*. *J. Plant Physiol.* **2021**, *260*, 153388. [CrossRef] [PubMed]
37. Jeong, H.J.; Kang, J.H.; Zhao, M.A.; Kwon, J.K.; Choi, H.S.; Bae, J.H.; Lee, H.A.; Joung, Y.H.; Choi, D.; Kang, B.C. Tomato *Male sterile* 10^{35} is essential for pollen development and meiosis in anthers. *J. Exp. Bot.* **2014**, *65*, 6693–6709. [CrossRef] [PubMed]
38. Hu, M.; Bai, M.; Yang, M.; Wu, H. Cell polarity, asynchronous nuclear divisions, and bidirectional cytokinesis in male meiosis in *Magnolia denudata*. *Protoplasma.* **2021**, *258*, 621–632. [CrossRef]
39. Wu, H.; Hu, M.L.; Yang, M. *Nymphaea colorata*, another basal angiosperm species with bidirectional cytokinesis in microsporogenesis. *Plant Signal. Behav.* **2021**, *16*, 1559–2316. [CrossRef]
40. Sannier, J.; Nadot, S.; Forchioni, A.; Harley, M.; Albert, B.; Harley, M. Variation in the microsporogenesis of monosulcate palm pollen. *Bot. J. Linn. Soc.* **2006**, *151*, 93–102. [CrossRef]
41. Blakmore, S.; Wortley, A.H.; Skvarla, J.J.; Rowley, J.R. Pollen wall development in flowering plants. *New Phytol.* **2007**, *174*, 483–498. [CrossRef]
42. Matamoro-Vidal, A.; Prieu, C.; Furness, C.A.; Albert, B.; Gouyon, P.H. Evolutionary stasis in pollen morphogenesis due to natural selection. *New Phytol.* **2016**, *209*, 376–394. [CrossRef]
43. Albert, B.; Raquin, C.; Prigent, M.; Nadot, S.; Brisset, F.; Yang, M.; Ressayre, A. Successive microsporogenesis affects pollen aperture pattern in the tam mutant of *Arabidopsis thaliana*. *Ann. Bot.* **2011**, *107*, 1421–1426. [CrossRef]
44. Walker, J.W.; Doyle, J.A. Bases of angiosperm phylogeny-palynology. *Ann. Mo. Bot. Gard.* **1975**, *62*, 664–723. [CrossRef]
45. Ressayre, A.; Dreyer, L.; Triki-Teurtroy, S.; Forchioni, A.; Nadot, S. Post-meiotic cytokinesis and pollen aperture pattern ontogeny: Comparison of development in four species differing in aperture pattern. *Am. J. Bot.* **2005**, *92*, 576–583. [CrossRef]
46. Albert, B.; Matamoro-Vidal, A.; Prieu, C.; Nadot, S.; Till-Bottraud, I.; Ressayre, A.; Gouyon, P.H. A review of the developmental processes and selective pressures shaping aperture pattern in Angiosperms. *Plants* **2022**, *11*, 357. [CrossRef] [PubMed]
47. Furness, C.A.; Rudall, P.J. Pollen and anther characters in monocot systematics. *Grana* **2001**, *40*, 17–25. [CrossRef]
48. Toghranegar, Z.; Nadot, S.; Albert, B. Variation of microsporogenesis in monocots producing monosulcate pollen grains. *Ann. Bot.* **2013**, *112*, 135–139. [CrossRef]
49. Periasamy, K.; Thangavel, S. Anther development in *Xylopia nigricans*. *Proc. Indian Acad. Sci.* **1988**, *98*, 251–255. [CrossRef]
50. Locke, J.F. Microsporogenesis and cytokinesis in *Asimina triloba*. *Bot Gaz.* **1936**, *98*, 159–168. [CrossRef]
51. Gabarayeva, N.I. Sporoderm development in *Asimina triloba* (*Annonaceae*). *Grana* **1992**, *31*, 213–222. [CrossRef]
52. Gabarayeva, N.I. Sporoderm Development in *Asimina triloba* (*Annonaceae*). II. The developmental events after callose dissolution. *Grana* **1993**, *32*, 210–220. [CrossRef]
53. Taylor, M.L.; Hudson, P.J.; Rigg, J.M.; Strandquist, J.N.; Schwartz, G.J.; Thiemann, T.C.; Osborn, J.M. Pollen ontogeny in *Victoria* (Nymphaeales). *Int. J. Plant Sci.* **2013**, *174*, 1259–1276. [CrossRef]
54. Sarwar, A. Ontogenetic development of pollen tetrads in *Vaccinium smallii* A. Gray (Ericaceae). *Jpn. J. Palynol.* **2012**, *58*, 61–71.